presented in this paper, in our opinion there is no doubt that these complexes exist, that their composition is $Tl(CN)_n^{3-n}$, $n = 1-4$, and that they are extremely strong and stable. We are not able to find any good explanation why these complexes have not been established before in spite of the possibility to investigate this system by means of, e.g., emf measurements. The equilibria between the complexes are fast (on the real time scale), and it is not a difficult task to find a good thallium- and/or cyanide-sensitive electrode. There might be a possibility that the well-known toxicity of cyanide and thallium has had a prohibitive effect on presumptive investigators. On the other hand, it was pointed out already by Ostwald by 1897, who discussed the high stability of cyanomercaurate species, that "notwithstanding the extremely poisonous character of its constituents, it exerts no appreciable poison effect".[6b] Another possibility might be that the presumed reduction of Tl(III) by cyanide, suggested in an authoritative source of information on thallium chemistry,[2] prevented chemists from looking into this chemical system.

In spite of the fact that a large number of cyanide compounds have been prepared and investigated by different methods, there is lack of reliable thermodynamic studies concerning the stability of the complexes in solution, as was shown in the recent review article by Beck.[4] Because of the importance of the cyanide ion and its complexes in chemistry and in chemical industry (e.g., cyanide process for leaching of noble metals), it seems worthwhile to continue investigations of metal-ion cyanide complexes. The multinuclear NMR technique seems to be a useful tool for this purpose.

Acknowledgment. The authors are grateful to The Swedish Natural Sciences Research Council (NFR) for financial support and, together with The Knut and Alice Wallenberg Foundation, for providing funds for purchasing the NMR spectrometers. We are also grateful to Dr. L. Andersson (KTH) and Dr. K. Holmström as well as I. Andersson and Dr. L. Pettersson (University of Umeå) for help with initial calculations using the LAKE computer program. We thank Prof. L. Eberson (University of Lund) for drawing our attention to one-electron redox reactions and Dr. I. Toth (University of Debrecen, Hungary) for help with the pH measurements. We are also indebted to Dipl. Chem. Maria Csertö for chemical analysis of the solutions.

Registry No. HCN, 74-90-8; ^{205}Tl, 14280-49-0; ^{13}C, 14762-74-4.

Synthesis and Electrochemical Studies of Catenates: Stabilization of Low Oxidation States by Interlocked Macrocyclic Ligands

Christiane Dietrich-Buchecker,*,† Jean-Pierre Sauvage,*,† and Jean-Marc Kern*,‡

Contribution from the Laboratoire de Chimie Organo-Minérale, UA au CNRS 422, Institut de Chimie, 1 rue Blaise Pascal, 67000 Strasbourg, France, and Laboratoire d'Electrochimie Organique, Institut de Chimie, 1 rue Blaise Pascal, 67000 Strasbourg, France.
Received December 19, 1988

Abstract: The coordinating properties of a catenand, consisting of two interlocked 30-membered rings, have been studied. Several complexes, the catenates, have been prepared and fully characterized. The electron spectra of catenates have been measured, showing intense absorption bands in the visible for the Cu^I and Ni^I complexes. The strong color of copper(I) and nickel(I) catenates corresponds to a metal-to-ligand charge-transfer (MLCT) transition. Many of the catenates studied are strong photoemitters, the excitation light being in the near-UV or visible region. Both ligand-localized or MLCT excited states are responsible for the emission properties observed, depending on the metallic species complexed. The two 2,9-diphenyl-1,10-phenanthroline (dpp) subunits, which form the complexing species of the catenand, adopt an "entwined" geometry in all the catenates isolated. This special shape was clearly demonstrated by ^1H NMR studies for copper(I), silver(I), zinc(II), and cadmium(II) catenates and for their corresponding acyclic analogues containing two 2,9-di-*p*-anisyl-1,10-phenanthroline (dap) chelates. The molecular topography of the system in solution is thus in perfect agreement with the solid-state structure of copper(I) catenate, as earlier determined by X-ray crystallography. A detailed electrochemical study of the various catenates prepared has been carried out. The very general trend is that low oxidation states of transition-metal catenates are strongly stabilized. Some one-electron reductive processes have clearly been shown to occur on the ligand without decomposition of the complex. This is the case for lithium(I), copper(I), and zinc(II) catenates. It is even possible to generate stable solutions of the anionic copper complex by two-electron reduction of copper(I) catenate. In other instances, electron transfer takes place on the metal. The most straightforward situation is that of Ni^{II}, which is very readily reduced to Ni^I (d^9), this monovalent nickel catenate being surprisingly stable toward reoxidation. The nature of the orbitals involved in the reduction of Fe^{II}, Co^{II}, Ag^I, and Cd^{II} (ligand or metal centered) is not certain as yet. In any case, the destabilizing effect toward high oxidation states was so pronounced that it turned out to be impossible to generate trivalent states like Fe^{III} or Co^{III}. Rather, oxidation of the ligand part ($E > 1.4$ V versus SCE) was observed.

A new class of ligands, the **catenands**, has recently been developed.[1-4] A catenand consists of two or several interlocked coordinating macrocycles, the first member of this series containing two 30-membered rings. The particular class of catenands that has been synthesized and studied in our laboratories displays special coordinating properties due to the geometrical features of the ligands and their corresponding complexes. For clarity, we will consider two sets of geometrical properties: **topography** and **topology**.

† Laboratoire de Chimie Organo-Minérale.
‡ Laboratoire d'Electrochimie Organique.

(1) Dietrich-Buchecker, C. O.; Sauvage, J. P.; Kintzinger, J. P. *Tetrahedron Lett.* **1983**, *24*, 5095.
(2) Dietrich-Buchecker, C. O.; Sauvage, J. P.; Kern, J. M. *J. Am. Chem. Soc.* **1984**, *106*, 3043.
(3) Sauvage, J. P. *Nouv. J. Chim.* **1985**, *9*, 299.
(4) Dietrich-Buchecker, C. O.; Sauvage, J. P. *Chem. Rev.* **1987**, *87*, 795.

0002-7863/89/1511-7791$01.50/0

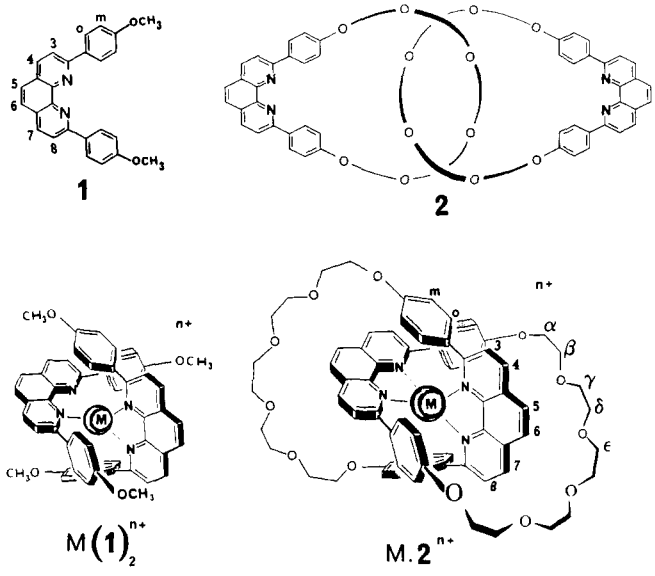

Figure 1.

(i) The topographical properties of a complex are related to the shape of the molecule and to bond lengths and angles within the coordination site.

(ii) The topological properties of a ligand—and, as a consequence, its corresponding complexes—are determined by its molecular graph. These properties are not associated with molecular shape but depend only on the number of interlocking rings.

The special arrangement of the coordinating fragments that form the complexing core is due to the nature of these fragments: 2,9-diphenyl-1,10-phenanthroline (dpp). By complexation to a metal, two dpp subunits lock together, while binding the metal, adopting an entwined topography. The highly rigid and encaging system thus obtained favors distorted tetrahedral geometries. The aromatic character of the ligands and their strong π-accepting ability together with the preferred shape of catenates are expected to highly stabilize low oxidation states, for two different reasons: the first factor, π-accepting character of the coordinating subunits, is really stabilizing, whereas the second factor corresponds to a strong destabilization of high oxidation states, due to the poor ligand field of tetrahedral geometry[5] and to steric factors that disfavor 5-coordinate complexes. The topography of the system is thus such that low oxidation states will be preferred to high valence states. The stability of the complexes (kinetic and thermodynamic) will now be ensured by the topology of the ligand: the interlocking of the rings prevents the dpp subunits from parting and thus greatly contributes to inhibiting the dissociation of the complexes. Thus, complexes of unusually low valent states may be made and isolated with interlocked ligands, whereas the corresponding acyclic dpp complexes are too labile to be studied.

We now report here the preparation of various catenates (Cu^{I}, Li^{I}, Fe^{II}, Co^{II}, Ni^{II}, Ag^{I}, Zn^{II}, and Cd^{II}) made from the original interlocked macrocyclic coordinating system, the catenand **2**. Some particular spectral properties (^{1}H NMR and absorption and emission electronic spectra) related to the special shape of the entwined geometry of the complexes are also described as well as a detailed electrochemical study.

The ligands used in the present study are presented in Figure 1 as well as the general shapes of the complexes. The latter adopts an "entwined topography", referring to the special arrangement found for the two dpp subunits. This particular geometry was found by X-ray crystallography in the solid state of various catenates.[6-8] It is also kept in solution, as shown by NMR studies.

For comparison, 2,9-di-*p*-anisyl-1,10-phenanthroline, **1** (dap), which can be considered as the acyclic analogue of cat-30, has also been studied. In particular, its ability to stabilize low oxidation states has been tested in parallel to that of **2**. Comparison of **1** and **2** complexes will allow direct estimation of the topological factors since the geometry around the complexed species M is likely to be virtually identical for $M(\mathbf{1})_2$ and $M\cdot\mathbf{2}$.

Experimental Section

Materials and Methods. Acetonitrile was dried and purified by distillation over CaH_2. $Cu(CH_3CN)_4BF_4$ was prepared by the literature method.[9] Alternatively, $Cu(CH_3CN)_4BF_4$ was prepared by reduction of $Cu(BF_4)_2$ (Ventron) by copper powder (excess) in CH_3CN under argon at room temperature, the mixture being stirred until complete bleaching of the solution was effected. It was then filtered and evaporated to dryness. This latter method was found to be more convenient than the previously published one.[9] All other chemicals were of reagent grade and were used without further purification.

^{1}H NMR spectra were recorded with a Bruker WP 200 SY spectrometer. Electronic spectra were performed with a Varian Cary 118 spectrometer or with a Kontron Unikon 80 one.

Emission spectra were obtained with a Shimadzu RF 450 spectrometer. The solutions were degassed by three freeze–thaw–pump cycles.

Melting points were measured with a Reichert micromelting point apparatus (uncorrected).

Preparation of the Ligands. Both ligands **1** and **2** were prepared as previously reported.[2,10,11]

Preparation of the Copper(I) Complex $Cu(\mathbf{1})_2^+$. For the preparation of $[Cu(\mathbf{1})_2^+][BF_4^-]\cdot H_2O$, the following experimental procedure was used: by the double-ended needle technique, 0.55 mmol (172 mg) of $[Cu(CH_3CN)_4^+][BF_4^-]$ in 30 mL of degassed acetonitrile was added under argon and at room temperature to a stirred solution of **1** (1 mmol, 392 mg) in 50 mL of degassed CH_2Cl_2. The mixture turned dark red immediately. After the solution was stirred for 2 h under argon at room temperature, the mixture was evaporated to dryness: dark-red needles of crude $Cu(\mathbf{1})_2^+$ are obtained in quantitative yield. The crude material was filtered through SiO_2 (CH_2Cl_2, 2% MeOH) and recrystallized from CH_2Cl_2–benzene, affording an analytical sample. Yield, 446 mg (94%).

$[Cu(\mathbf{1})_2^+][BF_4^-]\cdot H_2O$: mp 288–289 °C. Anal. Calcd for $C_{52}H_{42}N_4O_5CuBF_4$: C, 65.52; H, 4.41; N, 5.88; Cu, 6.67. Found: C, 65.49; H, 4.28; N, 6.07; Cu, 7.14.

Preparation of the Copper(I) Complex $Cu\cdot\mathbf{2}^+$. The synthesis of $[Cu\cdot\mathbf{2}^+][BF_4^-]$ has been described previously.[1,2] $[Cu\cdot\mathbf{2}^+][BF_4^-]$ was also prepared by mixing stoichiometric amounts of **2** and $[Cu(CH_3CN)_4^+][BF_4^-]$, the experimental procedure being similar to the one given for $Cu(\mathbf{1})_2^+$.

$[Cu\cdot\mathbf{2}^+][BF^{4-}]$: mp 274–275 °C. Anal. Calcd for $C_{68}H_{68}N_4O_{12}CuBF_4$: C, 63.65; H, 5.30; N, 4.37; Cu, 4.91. Found: C, 63.46; H, 5.39; N, 4.41; Cu, 4.84.

Preparation of the Copper(II) Complex $Cu\cdot\mathbf{2}^{2+}$. $Cu(ClO_4)_2\cdot 6H_2O$ (0.12 mmol, 46 mg) dissolved in 10 mL of MeOH was added at room temperature with stirring to a solution of **2** (0.1 mmol, 113 mg) in 30 mL of CH_2Cl_2. A dark-green color appeared immediately. After the solution stood for 5 days in the dark at room temperature, dark-green crystals were observed. The crystals were removed from the mother liquor by filtration on paper and dried under vacuum. Yield, 122 mg (85%).

$[Cu\cdot\mathbf{2}^{2+}][(ClO_4^-)_2]\cdot 2H_2O$: mp 265–267 °C. Anal. Calcd for $C_{68}H_{72}N_4O_{22}CuCl_2$: C, 57.04; H, 5.03, N, 3.91. Found: C, 56.97; H, 4.92; N, 3.83.

Preparation of the Copper(II) Complex $Cu(\mathbf{1})_2^{2+}$. $Cu(ClO_4)_2\cdot 6H_2O$ (0.27 mmol, 100 mg) dissolved in 10 mL of MeOH was added at room temperature to a stirring solution of **1** (0.5 mmol, 196 mg) in 10 mL of CH_2Cl_2. Dark-green crystals appeared after the solution stood for 4 days at room temperature. The crystals were filtered on paper, washed with a few milliliters of MeOH, and dried under vacuum. Yield, 256 mg (95%).

Due to its instability, this complex could not be characterized: thin-layer chromatography analysis showed that $Cu(\mathbf{1})_2^{2+}$ decomposes readily to give free ligand **1** and the copper(I) complex, $Cu(1)_2$.

Preparation of the Silver(I) Complex $Ag\cdot\mathbf{2}^+$. By the double-ended needle technique, 0.149 mmol (29 mg) of $AgBF_4$ in 6 mL of benzene was

(5) Cotton, F. A.; Wilkinson, G. In *Advanced Inorganic Chemistry*, 4th ed.; Wiley: New York, 1980; p 641.

(6) Cesario, M.; Dietrich-Buchecker, C. O.; Guilhem, J.; Pascard, C.; Sauvage, J. P. *J. Chem. Soc., Chem. Commun.* **1985**, 244.

(7) Cesario, M.; Dietrich-Buchecker, C. O.; Edel, A.; Guilhem, J.; Kintzinger, J. P.; Pascard, C.; Sauvage, J. P. *J. Am. Chem. Soc.* **1986**, *108*, 6250.

(8) Dietrich-Buchecker, C. O.; Guilhem, J.; Khemiss, A. K.; Kintzinger, J. P.; Pascard, C.; Sauvage, J. P. *Angew. Chem., Int. Ed. Engl.* **1987**, *26*, 661.

(9) Meerwein, H.; Hederick, V.; Wunsderlich, K. *Arkiv. Pharm.* **1958**, *291*, 541.

(10) Dietrich-Buchecker, C. O.; Marnot, P. A.; Sauvage, J. P. *Tetrahedron Lett.* **1982**, *23*, 5291.

(11) Dietrich-Buchecker, C. O.; Sauvage, J. P. *Tetrahedron Lett.* **1983**, *24*, 5091.

added to a stirred solution of **2** (0.125 mmol, 141 mg) in 4 mL of CH_2Cl_2. After mixing, the solution remained colorless. After the solution stood overnight in the dark, white crystals appeared. They were filtered on paper, washed with 5 mL of benzene, and dried under vacuum. Yield, 134 mg (80%).

[Ag·2$^+$][BF_4^-]·H_2O: mp 242–243 °C. Anal. Calcd for $C_{68}H_{70}N_4O_{13}AgBF_4$: C, 60.67; H, 5.24; N, 4.16. Found: C, 60.68; H, 5.01; N, 4.09.

Preparation of the Silver(I) Complex Ag(1)$_2^+$. By a procedure analogous to that described for Ag·2$^+$, 0.25 mmol (49 mg) of $AgBF_4$ in 6 mL of benzene was added to 0.5 mmol (196 mg) of **1** in 6 mL of CH_2Cl_2. Precipitation of colorless crystals occurred immediately. After the solution stood overnight, the crystals were filtered on paper, washed with 5 mL of benzene, and dried under vacuum. Yield, 159 mg (65%).

[Ag(1)$_2^+$][BF_4^-]: mp 189–190 °C. Anal. Calcd for $C_{52}H_{40}N_4O_4AgBF_4$: C, 63.75; H, 4.12; N, 5.72. Found: C, 63.86; H, 4.11; N, 5.75. Both silver(I) complexes of **2** and **1** might be recrystallized from CH_2Cl_2–benzene. It is noteworthy that both are stable in sunlight; no darkening was observed after a few days.

Preparation of the Cobalt(II) Complex Co·2^{2+}. $Co(ClO_4)_2·6H_2O$ (0.11 mmol, 40 mg) in 2 mL of CH_3CN was added with stirring at room temperature to a solution of **2** (0.10 mmol, 113 mg) in 2 mL of CH_2Cl_2. A bright-orange color appeared instantaneously. After the solution stood overnight, 50 mL of EtOH was slowly added to the solution: a dark-orange solid began to precipitate. Crude Co·2^{2+} was filtered after 24 h and dried under vacuum. Yield, 105 mg (75%). The complex could be recrystallized from CH_2Cl_2–toluene, affording an analytical sample.

[Co·2^{2+}][(ClO_4^-)$_2$]: mp 293–295 °C. Anal. Calcd for $C_{68}H_{68}N_4O_{20}CoCl_2$: C, 58.71; H, 4.93; N, 4.03. Found: C, 58.63; H, 4.80; N, 3.99.

Preparation of the Cobalt(II) Complex Co(1)$_2^{2+}$. An analogous procedure yielded 194 mg (74%) of bright-pink–orange crystals of compound Co(1)$_2^{2+}$ by mixing **1** (0.5 mmol, 196 mg) in 5 mL of CH_2Cl_2 and $Co(ClO_4)_2·6H_2O$ (0.25 mmol, 92 mg) in 4 mL of CH_3CN.

[Co(1)$_2^{2+}$][(ClO_4^-)$_2$]: mp 298–300 °C. Anal. Calcd for $C_{52}H_{40}N_4O_{12}CoCl_2$: C, 59.89; H, 3.87; N, 5.37. Found: C, 59.88; H, 3.84; N, 5.46.

Preparation of the Zinc(II) Complex Zn·2^{2+}. $Zn(ClO_4)_2·6H_2O$ (0.107 mmol, 40 mg) in 10 mL of ethanol was added with stirring at room temperature to a solution of **2** (0.10 mmol, 113 mg) in 10 mL of CH_2Cl_2. The mixture turned pale yellow rapidly. After the solution stood for 2 days, pale-yellow needles appeared. The needles were filtered on paper, washed with ethanol, and dried under vacuum. Yield, 125 mg (89%).

[Zn·2^{2+}][(ClO_4^-)$_2$]: mp 318–319 °C. Anal. Calcd for $C_{68}H_{68}N_4O_{20}ZnCl_2$: C, 58.44; H, 4.90; N, 4.01. Found: C, 58.20; H, 4.90; N, 3.95.

Attempt To Prepare the Zinc(II) Complex Zn(1)$_2^{2+}$. By a procedure analogous to the one above, Zn(1)$_2^{2+}$ could not be isolated: it decomposed readily to give the free ligand **1**.

Preparation of the Cadmium(II) Complex Cd·2^{2+}. $Cd(ClO_4)_2·6H_2O$ (0.12 mmol, 50 mg) in 5 mL of methanol was added at room temperature to a solution of **2** (0.062 mmol, 70 mg) in 5 mL of CH_2Cl_2. After 24 h, the pale-yellow solution was evaporated to dryness, and the crude compound was taken up in 50 mL of water and CH_2Cl_2 (1:1). The organic layer was carefully washed with water in order to remove excess cadmium salt, dried over $MgSO_4$, filtered, and evaporated to dryness. Yield, 92 mg of crude complex Cd·2^{2+} (quantitative). An analytical sample was obtained by recrystallization in CH_2Cl_2–benzene. Yield, 66 mg (74%) of very pale-yellow needles.

[Cd·2^{2+}][(ClO_4^-)$_2$]: mp 310–312 °C. Anal. Calcd for $C_{68}H_{68}N_4O_{20}CdCl_2$: C, 56.53; H, 4.74; N, 3.88. Found: C, 56.36; H, 4.72; N, 3.78.

Attempt To Prepare the Cadmium(II) Complex Cd(1)$_2^{2+}$. Addition of a large excess (0.286 mmol, 120 mg) of $Cd(ClO_4)_2·6H_2O$ in 5 mL of methanol to 0.25 mmol (98 mg) of **1** in 5 mL of CH_2Cl_2 led, by a procedure analogous to that described above, to 106 mg of crude complex Cd(1)$_2^{2+}$. The latter could only be detected by ^1H NMR; during the purification attempt, it decomposed to give **1**.

Preparation of the Lithium Complex Li·2$^+$. $LiBF_4$ (0.17 mmol, 16 mg) in 5 mL of methanol was added at room temperature to a solution of **2** (0.08 mmol, 90.6 mg) in 5 mL of CH_2Cl_2. After the solution stood overnight, the solvents were evaporated to dryness. Crude compound was redissolved in 30 mL of water and CH_2Cl_2 (1:1). After being washed with water, the organic layer was dried over $MgSO_4$, filtered, and evaporated. The very pale-yellow crude complex Li·2$^+$ was further recrystallized in CH_2Cl_2–benzene. Yield, 84 mg (85%).

[Li·2$^+$][BF_4^-]: mp 249–252 °C. Anal. Calcd for $C_{68}H_{68}N_4O_{12}LiBF_4$: C, 66.56; H, 5.58; N, 4.57. Found: C, 66.43; H, 5.50; N, 4.62.

Attempt To Prepare the Lithium Complex Li(1)$_2^+$. By a procedure analogous to the one described above, Li(1)$_2^+$ could not be prepared. After workup, only the free ligand **1** was isolated.

Electrochemistry. (a) Solvents and Supporting Electrolytes. CH_3CN, spectroscopic grade, was distilled over CaH_2 under argon and stored under argon. DMF, (dimethylformamide Prolabo, R.P. Normapur), was stirred with P_2O_5 overnight, filtered, distilled under reduced pressure, and stored under argon. CH_2Cl_2 (Chlorure de Méthylène, Prolabo, R.P. Normapur) was purified by percolation over neutral aluminum oxide (Merck). TEAP (tetraethylammonium perchlorate) and $TEABF_4$ (tetraethylammonium tetrafluoroborate) were prepared as previously described,[12] recrystallized twice in a H_2O–MeOH mixture, and dried 48 h under vacuum at 40 °C. TBAP (tetrabutylammonium perchlorate) (Fluka purum) was twice recrystallized in a H_2O–EtOH mixture and dried 48 h at 40 °C under vacuum.

(b) Instrumentation. Polarographic measurements were performed on a Tacussel polarograph (TIPOL-EPL2). The dropping mercury electrode (DME) characteristic of $m^{2/3}\,t^{1/6}$ was 2.51 in the absence of polarization. A Bruker EI 30 M potentiostat and a Ifelec IF 3802 recorder served for cyclic voltammetry measurements and controlled-potential electrolyses. In CH_3CN or DMF medium, a saturated calomel electrode (SCE) served as the reference electrode. It was separated from the test solution by an auxiliary compartment filled with the electrolytic solution. In CH_2Cl_2 solutions, a $Ag_3I_4^-Bu_4N^+/Ag$[13] electrode was used as reference. Its potential versus ferricinium/ferrocene was −0.625 V; its potential versus SCE in CH_2Cl_2 was −0.145 V.

A hanging mercury electrode (HME; Metrohm EA290), a platinum button electrode (A = 7 mm^2), a planar platinum electrode (A = 28 mm^2), and a planar glassy carbon electrode (A = 28 mm^2) were used for cyclic voltammetry. All experiments were done under argon atmosphere in a Metrohm universal recipient, in a three-electrode configuration.

Preparative and coulometric experiments were done in a 10-cm^3 cell, either with a stirred mercury pool (A = 200 mm^2) or with a coiled platinum wire ($l \simeq 30$ cm).

Results and Discussion

Preparation of Complexes: Absorption and Emission Electronic Spectra. The complexes were made by mixing stoichiometric amounts of metal salts (BF_4^- or ClO_4^-) and ligand in MeOH and CH_2Cl_2. All the catenates prepared were highly crystalline materials. The behavior of **1** and **2** turned out to be noticeably different with respect to the preparation of their respective complexes. Whereas isolation of catenates was straightforward, preparation of dap complexes turned out to be much more difficult.

Owing to the poor stability of some bis-dap complexes,[14] it was not possible to isolate and characterize them (Zn^{II}, Cd^{II}, Li^{I}, and Ni^{II}). At each attempt, free dap was recovered. However, bis-dap complexes of Cu^{I}, Cu^{II}, Ag^{I}, and Co^{II} could be crystallized as pure compounds.

The destabilizing effect of the anisyl groups of dap in alkali cation complexation with respect to unsubstituted 1,10-phenanthroline (phen) is evident. It was shown previously[15–17] that Li^+ forms isolable complexes with phen-type ligands. It it thus likely that isolation of a lithium catenate is allowed only because of favorable topological factors but that even within Li·2$^+$ the four phenyl groups borne by the phen rings also display destabilizing properties. Indeed Li·2$^+$ is readily decomplexed in a polar solvent like DMF, in agreement with the relatively poor stability of this catenate.

The cationic complexes made are listed in Table I as well as the most characteristic data of their electron spectra. The UV spectra are as expected for 1,10-phenanthroline derivative complexes. More interesting is the visible region. Copper(I) complexes show broad and intense metal-to-ligand charge-transfer (MLCT) bands, in agreement with previously studied systems containing ligand-localized low-lying π^* orbitals.[18–21] In addition, Zn^{II}, Cd^{II},

(12) House, H. O.; Feng, E.; Peet, N. *J. Org. Chem.* **1971**, *36*, 2371.
(13) Coutagne, D. *Bull. Soc. Chim. Fr.* **1971**, 1940.
(14) Arnaud-Neu, F.; Marques, E.; Schwing-Weill, M. J.; Dietrich-Buchecker, C. O.; Sauvage, J. P.; Weiss, J. *New J. Chem.* **1988**, *12*, 15.
(15) Pfeiffer, P.; Christeleit, W. *Z. Anorg. Allg. Chem.* **1938**, *239*, 133.
(16) Vögtle, F.; Müller, W. M.; Rasshofer, W. *Isr. J. Chem.* **1979**, *18*, 246.
(17) Constable, E. C.; Chung, L. Y.; Lewis, J.; Raithby, P. R. *J. Chem. Soc., Chem. Commun.* **1986**, 1719.
(18) Mc Millin, D. R.; Buckner, M. T.; Ahn, B. T. *Inorg. Chem.* **1977**, *16*, 943.
(19) Dietrich-Buchecker, C. O.; Marnot, P. A.; Sauvage, J. P.; Kirchhoff, J. R.; Mc Millin, D. R. *J. Chem. Soc., Chem. Commun.* **1983**, 513.

Table I. Absorption and Emission Electronic Properties

compd	absorption,[a] λ_{max}(nm) [log ϵ]	emission[a] λ_{ex},[b] nm	emission[a] λ_{em},[c] nm
1	240 [4.46], 285 [4.66], 323 [4.41], 340 [4.39]	288	398
2	227 [4.69], 240 [4.77], 285 [4.88], 321 [4.62], 342 [4.55] sh	322	398
$Cu(\mathbf{1})_2^+$	235 [4.85], 245 [4.85], 280 [4.77], 331 [4.74], 436 [3.48], sh near 475 and 600	470	695
$Cu\cdot\mathbf{2}^{2+}$	235 [4.74], 255 [4.73], 300 [4.60], 360 [4.66], 700 [3][d]	*e*	*e*
$Cu\cdot\mathbf{2}^{+}$	248 [4.85], 275 [4.76], 323 [4.68], 440 [3.48], sh near 475 and 600	470	680
$Cu\cdot\mathbf{2}^{2+}$	253 [4.67], 275 [4.59], 302 [4.53], 347 [4.50], 470 [2.88], 685 [2.90][d]	*e*	*e*
$H\cdot\mathbf{2}^{+}$	238 [4.79], 274 [4.73], 301 [4.65], 342 [4.47] sh	322	397
$Ag(\mathbf{1})_2^+$	238 [4.99], 286 [4.95], 325 [4.81], 337 [4.80] sh	359	400
$Ag\cdot\mathbf{2}^{+}$	240 [4.89], 279 [4.74], 311 [4.68]	280	384
$Zn(\mathbf{1})_2^{2+}$	234 [4.86], 251 [4.81], 292 [4.75], 310 [4.72] sh, 354 [4.72]	365	463
$Zn\cdot\mathbf{2}^{2+}$	235 [4.72], 251 [4.72], 277 [4.59], 292 [4.61], 310 [4.60], 346 [4.57]	355	461
$Cd\cdot\mathbf{2}^{2+}$	236 [4.95], 249 [4.89] sh, 266 [4.75], 289 [4.75], 328 [4.72]	342	437
$Li\cdot\mathbf{2}^{+}$	238 [4.85], 279 [4.77], 324 [4.69]	332	400
$Co(\mathbf{1})_2^{2+}$	237 [4.78], 248 [4.73] sh, 293 [4.66], 342 [4.65]	347	424
$Co\cdot\mathbf{2}^{2+}$	233 [4.90], 249 [4.80], 298 [4.69] sh, 310 [4.69], 501 [2.89]	342	435
$Ni(\mathbf{1})_2^{2+}$	250 [4.72], 286 [4.63], 336 [4.62]	*e*	*e*
$Ni\cdot\mathbf{2}^{2+}$	228 [4.72], 250 [4.62], 318 [4.46]	360	450
$Ni\cdot\mathbf{2}^{+}$	255 [4.81], 283 [4.73], 328 [4.69], 645 [3.68]	365	402

[a] In CH_2Cl_2. [b] This wavelength was chosen as the excitation spectrum maximum. [c] Uncorrected value. [d] In the visible range, λ_{max} = 666 nm for $Cu(\mathbf{1})_2^{2+}$ and $Cu\cdot\mathbf{2}^{2+}$ in acetonitrile. [e] Not measured.

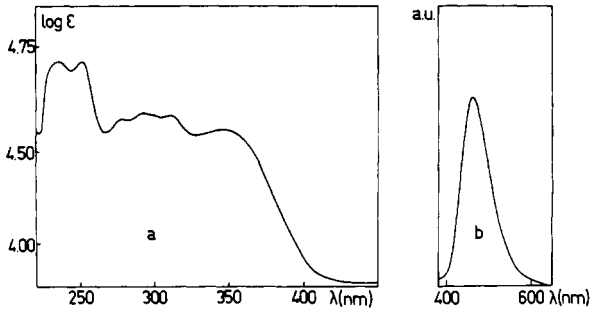

Figure 2. Absorption (a) and emission (b) of $[Zn\cdot\mathbf{2}^{2+}][ClO_4^-]_2$ (9.1×10^{-6} mol L^{-1}) in CH_2Cl_2; for (b), the excitation wavelength is λ_{exc} = 355 nm.

and Ag^I complexes, $H\cdot\mathbf{2}^{+}$, and $Li\cdot\mathbf{2}^{+}$ are yellow. A participation of the intramolecular charge-transfer interactions (phenoxyphenanthroline) to the low-energy bands found in the absorption spectrum of the latter compounds might account for this observation.

Copper(I) complexes luminesce from their MLCT excited state, as previously reported.[18-22] In addition, the other complexes prepared are strong emitters when excited by near-UV light ($\lambda_{exc} \sim 360$ nm). This property is in agreement with the luminescence data described earlier for 1,10-phenanthroline[23] and some of its complexes.[24,25] In particular, $Zn\cdot\mathbf{2}^{2+}$ displays very intense luminescence (λ_{em} = 461 nm) in CH_2Cl_2 solution when excited at 355 nm, as shown in Figure 2. The luminescence properties of some catenates may be interesting for photophysical and photochemical applications.

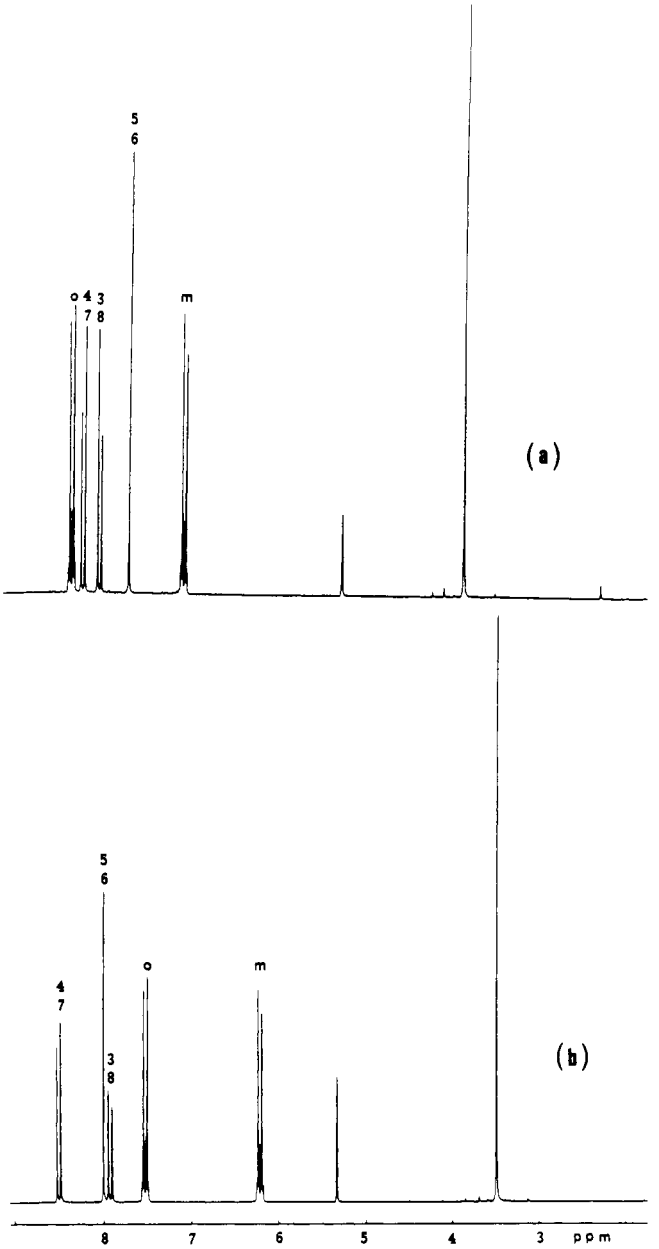

Figure 3. 200-MHz ^1H NMR spectra of **1** (a) and $Ag(\mathbf{1})_2^+$ (b) in CD_2Cl_2.

^1H NMR Spectroscopy Studies: Demonstration of the Entwined Topography of All the Catenates Studied in Solution. ^1H NMR data for free ligands **1** and **2** and for some of their complexes are shown in Table II. As observed previously for $Cu\cdot\mathbf{2}^{+}$,[1,2] $Cu(\mathbf{1})_2^+$,[22] and $H\cdot\mathbf{2}^{+}$,[7] the entwined topography of the molecular system is evidenced by the typical proton chemical shifts. The two coordinating dpp subunits of **2** are remote from one another in the free ligand, and their corresponding protons show normal chemical shift values, close to those observed for **1** (see Table II). On the other hand, the system undergoes a complete rearrangement during the complexation process that brings the two dpp fragments to close proximity either in $M(\mathbf{1})_2^{n+}$ or $M\cdot\mathbf{2}^{n+}$ (M^{n+} is the complexed cationic species). The dpp subunits fit together in the complexes, leading to an "entwined topography". As a consequence, some particular protons like H_o, H_m, and $CH_{2,\alpha}$ become located above and below the 1,10-phenanthroline nuclei. Due to intense ring

(20) Mc Millin, D. R.; Kirchhoff, J. R.; Goodwin, K. V. *Coord. Chem. Rev.* **1985**, *64*, 83.
(21) Ichinaga, A. K.; Kirchhoff, J. R.; Mc Millin, D. R.; Dietrich-Buchecker, C. O.; Marnot, P. A.; Sauvage, J. P. *Inorg. Chem.* **1987**, *26*, 4290.
(22) Dietrich-Buchecker, C. O.; Marnot, P. A.; Sauvage, J. P.; Kintzinger, J. P.; Maltèse, P. *Nouv. J. Chim.* **1984**, *8*, 573.
(23) Brinen, J. S.; Rosebrook, D. D.; Hirt, R. C. *J. Phys. Chem.* **1963**, *67*, 2651.
(24) Halper, W.; De Armond, M. K. *Chem. Phys. Lett.* **1974**, *24*, 114.
(25) Ohno, T.; Kato, S. *Bull. Chem. Soc. Jpn.* **1984**, *57*, 3391.

Table II. ^{1}H NMR Spectra of **1**, **2**, and Their Complexes: δ (ppm) in CD_2Cl_2[a]

compd	$H_{4,7}$	$H_{5,6}$	$H_{3,8}$	H_o	$\Delta\delta$[b] on H_o	H_m	$\Delta\delta$[b] on H_m	CH_3	H_ϵ	H_α, H_β, H_γ, H_δ
1	8.30	7.78	8.11	8.43		7.14		3.92, s		
2	8.29	7.78	8.11	8.49		7.11			3.70, s	4.20, t; 3.62–3.74, m
$Cu(\mathbf{1})_2^+$	8.47	8.01	7.86	7.44	−0.99	6.06	−1.08	3.45, s		
$Cu\cdot\mathbf{2}^+$	8.66	8.28	7.87	7.37	−1.12	6.02	−1.09		3.82, s	3.67, 3.60, 3.50, m
$Ag(\mathbf{1})_2^+$	8.49	7.99	7.92	7.52	−0.91	6.21	−0.93	3.48, s		
$Ag\cdot\mathbf{2}^+$	8.81	8.25	7.92	7.26	−1.23	6.09	−1.02		3.77, s	3.55, 3.22, m
$Zn\cdot\mathbf{2}^{2+}$	9.00	8.57	8.09	7.29	−1.20	6.23	−0.88		3.84, s	3.80, 3.70, 3.62, m
$Cd(\mathbf{1})_2^{2+}$	8.78	8.19	8.10	7.28	−1.15	6.38	−0.76	3.52, s		
$Cd\cdot\mathbf{2}^{2+}$	9.14	8.49	8.14	7.18	−1.31	6.31	−0.80		3.79, s	3.62, 3.40, m
$Li\cdot\mathbf{2}^+$	8.63	8.20	7.77	7.23	−1.26	6.06	−1.05		3.80, s	3.66, 3.54, m

[a] Internal reference: $CDHCl_2$ at 5, 32 ppm. $H_{5,6}$ leads to a singlet; $H_{3,8}$ and $H_{4,7}$ show an AB pattern (coupling constant $J \simeq 8.5$ Hz), whereas H_o and H_m give rise to AA'XX' systems ($J \simeq 8.7$ Hz). [b] $\Delta\delta$ is defined as the chemical shift of a given proton (H_o or H_m) in the free liggand − the chemical shift of this same proton in the corresponding complex.

current effects, the corresponding resonance signals move to higher field as compared to their positions in the free-ligand spectra. Lithium(I) catenate is a typical example. The H_o, H_m, and $H_{CH_{2\alpha}}$ signals are shifted upfield by complexation: −1.26, −1.05, and −0.54 ppm, respectively. Other representative spectra are given in Figures 3 and 4.

Noteworthy is the strong complexing ability of **2** as compared to **1**. In agreement with the difficulty or impossibility in isolating some complexes of **1**, ^{1}H NMR studies show that those complexes are also unstable in polar media. In several cases, the corresponding complexes of **2** could easily be observed and studied by ^{1}H NMR. The most striking example is the lithium complex: **1** does not show significant complexing ability toward Li^+, whereas **2** forms a stable lithium complex in a variety of solvents. Those observations have recently been confirmed by a detailed stability constant study.[14]

Dinuclear complexes containing one cationic species per dpp species have never been observed either by NMR spectroscopy or by any other method.[26]

Electrochemical Study. 2,2'-Bipyridine (bipy) and phen-type ligands have been used for many years to stabilize various oxidation states of transition metals. Many studies have been devoted to the elucidation of the electrochemical properties of bipy and phen complexes, as shown by the numerous examples cited in the excellent review of McWhinnie and Miller.[27] The propensity of aromatic polyimine chelates to stabilize the low oxidation state was recognized long ago. The most studied cases are probably those of Fe^{II} and Cu^{I}. For the former, the stability of the tris-bipy complex was demonstrated in particular by the high redox potential of the Fe^{III}/Fe^{II} couple (+1.026 V/NHE in 1 M H_2SO_4[28] and 1.012 V/SCE in CH_3CN[39]).

The question related to the oxidation number of the transition metal in certain highly reduced compounds was also addressed a long time ago.[27,29] It was noticed that, in particular, the 18-electron rule was no longer valid for a variety of complexes.[30] Clearly, complexes of metals in formally negative or zero oxidation states are in some cases best regarded as complexes of the ligand anion. Some important examples of true zero-valent complexes are carbonyl complexes like $M(bipy)(CO)_4$ (M = Cr, Mo, and W)[32] and $V(bipy)_3$.[31] Catenand **2** and its acyclic analogue **1** contain strong π-acceptor ligands of the phen type and are thus expected to behave as discussed above. In addition, a very important characteristic of **2** and, to a lesser extent, of **1** is of geometrical origin. The presence of bulky substituents α to the nitrogen atoms of the constitutive chelates of **1** and **2** inhibits the formation of octahedral complexes but favors tetrahedral geometries. This property was already evidenced in the past for 2,9-dimethyl-1,10-phenanthroline complexes,[33] and in particular, it

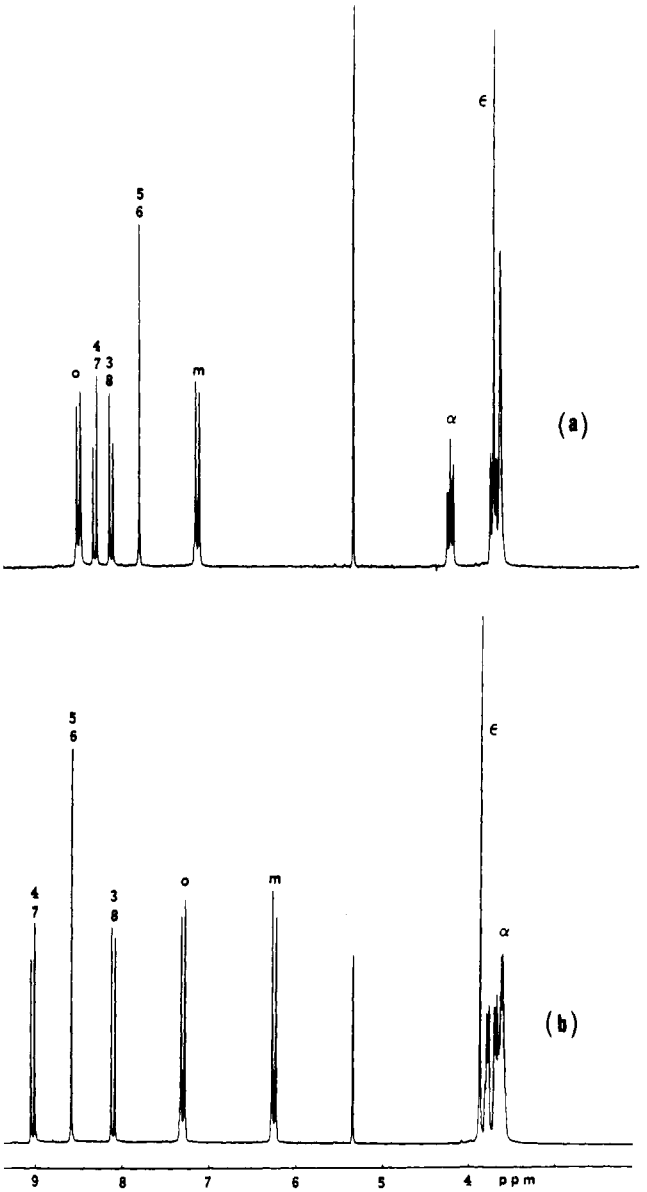

Figure 4. 200-MHz ^{1}H NMR spectra of **2** (a) and $Zn\cdot\mathbf{2}^{2+}$ (b) in CD_2Cl_2.

(26) Albrecht-Gary, A. M.; Dietrich-Buchecker, C. O.; Saad, Z.; Sauvage, J. P. *J. Am. Chem. Soc.* **1988**, *110*, 1467.
(27) McWhinnie, W. R.; Miller, J. D. *Adv. Inorg. Radiochem.* **1969**, *12*, 135.
(28) Schilt, A. A. *Anal. Chem.* **1963**, *35*, 1599.
(29) (a) Cotton, F. A.; Wilkinson, G. In *Advanced Inorganic Chemistry*, 4th ed.; Wiley Interscience: New York, 1980; pp 119–121. (b) Schilt, A. A. In *Applications of 1,10 Phenanthroline and related Compounds*; Pergamon: London, 1969.
(30) Cotton, F. A.; Wilkinson, G. In *Advanced Inorganic Chemistry*, 4th ed.; Wiley Interscience: New York, 1980.
(31) Kaizu, Y.; Yazaki, T.; Torii, Y.; Kobayashi, H. *Bull. Chem. Soc. Jpn.* **1970**, *43*, 2068.
(32) (a) Hieber, W.; Mühlbauer, F. *Z. Anorg. Allg. Chem.* **1935**, *221*, 337, 349. (b) Stiddard, M. H. B. *J. Chem. Soc.* **1962**, 4712.
(33) James, B. R.; Williams, R. J. P. *J. Chem. Soc.* **1961**, 2007.

Table III. Electrochemical Properties of Various Catenates and Their Acyclic Analogues: $E_{1/2}$ Values Determined by Cyclic Voltammetry or by Polarography[a]

	metal									
	Li		H	Fe		Co		Ni		
overall charge of the complex	+1/0,	0/−1	+1/0	+2/+1	+1/0	+2/+1	+1/0	+2/+1	+1/0	
medium	CH_3CN		CH_2Cl_2	CH_2Cl_2		CH_3CN		CH_3CN		
1	no complex			no complex		−0.600	−1.275	−0.160	−1.305	
2	−1.80,	−1.93 qr	−1.075[h] ir	−0.715	−1.260	−0.600	−1.315	−0.180	−1.325	
free metal	−1.965[c]			$E_{1/2}(Fe^{2+/0})$ = −1.00[e]		$E_{1/2}(Co^{2+/0})$ = −0.61/CH_3CN[f]		$E_{1/2}(Ni^{2+/0})$ = −0.29/CH_3CN[f]		

	metal								
	Cu			Zn		Ag	Cd		
overall charge of the complex	+2/+1	+1/0	0/−1	+2/+1	+1/0	+1/0	+2/0	+2/+1	+1/0
medium	CH_3CN	DMF		CH_2Cl_2		CH_3CN	CH_3CN	CH_2Cl_2	
1	+0.615[b]	−1.610[c]	−1.815[c]	−1.010 qr	−1.310 qr	+0.185[d]	−0.40[c,h] ir		
2	+0.565[b]	−1.650[c]	−1.860[c]	−0.960 qr	−1.260 qr	−0.70[d]	−0.91[c,h] ir	~−1.15[b] qr	~−1.35[b] qr
free metal	$E_{1/2}(Cu^{2+/+})$ = +1.05/CH_3CN[b,g] $E_{1/2}(Cu^{+/0})$ = −0.310/CH_3CN[c,f]; −0.530/CH_3CN[b,f]			$E_{1/2}(Zn^{2+/0})$ = −0.67/CH_2Cl_2[d] $E_{1/2}(Zn^{2+/0})$ = −0.62/CH_3CN[f]		+0.420[d]	−0.285[d]		

[a] All potentials refer to SCE; the systems are reversible except in a few cases indicated by qr (quasi-reversible) or ir (irreversible). The potentials have been determined by CV on both Pt and Hg, leading to identical values, except for the measurements marked *b*, *c*, or *d*, which have been made on only one type of electrode or by another method. [b] Pt electrode. [c] Hg electrode. [d] Polarography at the DME. [e] See ref 73. [f] See ref 75. [g] See ref 65. [h] Peak potential.

was taken advantage of for analytical purposes (copper(I)).[34,35] **1** bears two aromatic substituents which are responsible for the particular **entwined** geometry of its complexes, leading to highly encaged and rigid systems. In addition, the topological properties of **2** (interlocked ligands) inhibit separation of its two coordinating subunits while they are complexed to a given cationic species. This characteristic enables **2** to bind strongly to transition metals, even in their lowest oxidation states. Furthermore, **2** is able to complex transition metals even after having accepted one or two electrons, whereas **1** complexes dissociate much more readily upon exhaustive reduction. Here again, this is related to the different topological properties of both coordinating systems.

Some typical examples will be discussed below, with a particular emphasis on the comparison between the catenates and the analogous complexes of **1**. They include the electrochemical study of free ligands **1** and **2** and their complexes with Li^+ (for **2**), H^+ (for **2**), Fe^{2+} (for **2**), Co^{2+}, Ni^{2+}, Cu^+, Zn^{2+}, Ag^+, and Cd^{2+}.

The electrochemical study was performed mainly by cyclic voltammetry on a Pt or Hg electrode. Some measurements using the polarographic method were also carried out. Several solvents were used (CH_3CN, DMF, and CH_2Cl_2) owing to the poor solubility of **1** or **2** in CH_3CN, to the low stability of some complexes of **1** in DMF, and to the limited cathodic range of CH_2Cl_2. Furthermore, the choice of solvent has also been dictated by adsorption and passivation difficulties. Such problems have been encountered by others when they studied various phen complexes.[36] For instance, reduction of copper(I) catenate was best studied in DMF. Electrochemical data were obtained either from isolated crystalline complexes or from in situ generated complexes obtained by mixing the appropriate amounts of ligand and metal salt ($Ni(\mathbf{1})_2^{2+}$, $Zn(\mathbf{1})_2^{2+}$, and $Cd(\mathbf{1})_2^{2+}$). It has been checked that both methods lead to identical results, for instance in the cases of Co^{2+}, Cu^+, Ag^+, and Zn^{2+} complexes.

The electrochemical data are collected in Table III. All the redox potentials are given versus the saturated calomel electrode in volts. The redox processes observed in the course of the present study might involve either metal-centered reactions (d or s orbitals) or electron transfer to the organic ligand (π^* orbitals of the dpp subunits). In some cases, the assignment can be made via EPR measurements and redox potential values. If the Cu^{II}/Cu^{I} couple always involves a metal-centered redox process, the electron transfer to $Li\cdot\mathbf{2}^+$ clearly occurs on the ligand moiety. No distinction can be made between both pathways for many of the complexes studied.

(a) Free Ligands and the Lithium Complex of 2. **2** is insoluble in CH_3CN and could thus not been studied in this medium. However, **1** is fairly soluble and is expected to display identical electronic properties as **2**:

$$\mathbf{1} + e^- \rightleftharpoons \mathbf{1}^- \qquad E_{1/2} = -2.00 \text{ V}$$

$$\mathbf{1}^- + e^- \rightleftharpoons \mathbf{1}^{2-} \qquad E_{1/2} = -2.19 \text{ V}$$

$Li(\mathbf{1})_2^+$ could not be obtained even in solution, whereas the catenate $Li\cdot\mathbf{2}^+$ is stable in CH_3CN and shows two reduction waves, only the first one (−1.80 V) being reversible. Those electron transfers were observed on both Hg and Pt, at the same potential values. They correspond to reduction of the catenate:

$$Li\cdot\mathbf{2}^+ \underset{-e^-}{\overset{e^-}{\rightleftharpoons}} [Li^{\cdot+}\mathbf{2}^{\bullet-}]^0 \underset{-e^-}{\overset{e^-}{\rightleftharpoons}} [Li^{\cdot+}\mathbf{2}^{2-}]^-$$

Indeed, free Li^+ is reversibly reduced to Li–Hg at −1.96 V under identical conditions.

Electrolysis of $Li\cdot\mathbf{2}^+$ on a mercury pool or platinum wire at −1.90 V leads to buildup of a red species which subsequently decomposes in solution. This compound is likely to be the lithium-stabilized radical anion $[Li^+\cdot\mathbf{2}^-]^0$. The interlocking nature of **2** allows complexation of Li^+, whereas **1** is unable to form any stable complex. This same topological property permits the formation of highly reduced complexes of **2** with Li^+, the coordinating fragments being radical anions of the $dpp^{\bullet-}$ type. Ion pairs and radical complexes formed between $phen^{\bullet-}$ and alkali cations or phenylmagnesium have recently been examined by EPR measurements and from theoretical calculations.[37]

(b) Iron(II) Catenate. 2,9-Dimethyl-1,10-phenanthroline does not lead to a tris-chelate Fe^{II} complex.[38] However, $Fe\cdot\mathbf{2}^{2+}$ can be prepared, probably as a tetracoordinate complex. Reduction

(34) (a) Smith, G. F.; Mc Curdy, W. H., Jr. *Anal. Chem.* **1952**, *24*, 371. (b) Luke, C. L.; Campbell, M. E. *Anal. Chem.* **1953**, *25*, 1588. (c) Irving, H.; Mellor, D. H. *J. Chem. Soc.* **1962**, 5237. (d) Prabhu, S. V.; Baldwin, R. P.; Kryger, L. *Anal. Chem.* **1987**, *59*, 1074.

(35) (a) Guadalupe, A. R.; Abruna, H. D. *Anal. Chem.* **1985**, *57*, 142. (b) Wier, L. M.; Guadalupe, A. R.; Abruna, H. D. *Anal. Chem.* **1985**, *57*, 2009.

(36) (a) Gürther, O.; Dietz, K. P.; Thomas, Ph. *Z. Anorg. Allg. Chem.* **1973**, *396*, 217. (b) Musumeci, S.; Rizzarelli, E.; Fragalà, I.; Sammartano, S.; Bonomo, R. P. *Inorg. Chim. Acta* **1973**, *7*, 660.

(37) Kaim, W. *J. Am. Chem. Soc.* **1982**, *104*, 3833.

(38) (a) Fox, D. B.; Hall, J. R.; Plowman, R. A. *Aust. J. Chem.* **1962**, *15*, 235. (b) König, E.; Ritter, G. *J. Inorg. Nucl. Chem.* **1981**, *43*, 2273.

of the iron(II) catenate Fe·2^{2+} in CH_2Cl_2 occurs in two reversible steps on Pt or Hg:

$$Fe\cdot\mathbf{2}^{2+} + e^- \rightleftharpoons Fe\cdot\mathbf{2}^{+} \qquad E_{1/2} = -0.715\ V, \quad \Delta E_p = 60\ mV$$

$$Fe\cdot\mathbf{2}^{+} + e^- \rightleftharpoons Fe\cdot\mathbf{2}^{0} \qquad E_{1/2} = -1.260\ V, \quad \Delta E_p = 65\ mV$$

Between the two reversible systems mentioned above, a reduction peak is observed at $E_p = -1.07$ V. This peak corresponds to irreversible reduction of the proton catenate H·2^+,[7] the starting iron(II) complex Fe·2^{2+} being always contaminated by H·2^+ as confirmed by ^1H NMR. Indeed, formation of the proton catenate is surprisingly easy due to topological enhancement of the basicity of the catenand **2**.[7] For bipy and 2,2′:6′,2″-terpyridine (terpy) complexes of iron, the redox couples are as follows:[39,40]

$$Fe(bipy)_3^{2+} + e^- \rightleftharpoons Fe(bipy)_3^{+} \qquad E_{1/2} = -1.34\ V\ vs\ SCE\ in\ CH_3CN$$

$$Fe(bipy)_3^{+} + e^- \rightleftharpoons Fe(bipy)_3^{0} \qquad E_{1/2} = -1.53\ V$$

$$Fe(terpy)_2^{2+} + e^- \rightleftharpoons Fe(terpy)_2^{+} \qquad E_{1/2} = -1.25\ V$$

$$Fe(terpy)_2^{+} + e^- \rightleftharpoons Fe(terpy)_2^{0} \qquad E_{1/2} = -1.42V$$

By comparing the bipy and terpy systems to the iron catenate, it is obvious that considerable stabilization of the low oxidation states takes place in the interlocked system. For instance, the monovalent state of the iron catenate is highly accessible:

$$E_{1/2_{Fe\cdot\mathbf{2}^{2+/+}}} - E_{1/2_{Fe(bipy)_3^{2+/+}}} = +0.6\ V$$

For $Fe(bipy)_3^{2+}$ and $Fe(terpy)_2^{2+}$ reduction, the redox orbitals involved are clearly ligand localized.[31,41,42] In the case of Fe·2^{2+}, the situation is not so straightforward, and the redox process could very well involve the metal center, as previously reported for other Fe^{II}/Fe^{I} couples.[43-46]

The situation regarding the Fe^{III}/Fe^{II} couple is also of interest:

$$Fe(bipy)_3^{2+} \rightleftharpoons Fe(bipy)_3^{3+} + e^- \qquad E_{1/2} = +1.012\ V\ (CH_3CN)^{39}$$

$$Fe\cdot\mathbf{2}^{2+} \not\rightleftharpoons Fe\cdot\mathbf{2}^{3+} + e^- \qquad E_{1/2} > 1.40V$$

The metal-localized redox process $Fe(bipy)_3^{3+/2+}$ occurs at an accessible protenial, whereas Fe·2^{2+} could not be oxidized to Fe^{III}. Instead, it may be that oxidation of the ligand occurs before any oxidative process involving the iron(II) center takes place:

$$E_{1/2_{Fe\cdot\mathbf{2}^{3+/2+}}} - E_{1/2_{Fe(bipy)_3^{3+/2+}}} > 0.4\ V$$

It is remarkable that the trivalent state of the iron complex cannot be reached. If one compares Fe·2^{2+} to other iron complexes that do not contain diimine ligands of the bipy type, the effect is even more spectacular. The divalent state stabilization is close to 1 V as compared to aquo iron(II) ($Fe_{aquo}^{III/II}$: $E_{1/2} = +0.77$ V/NHE in 1 M HCl)[47] or ferrocyanide ($Fe(CN)_6^{3-/4-}$: $E_{1/2} = +0.69$ V/NHE in 1 N H_2SO_4).

Compared to the bipy complexes, the stabilization of low formal oxidation states of iron rests only on geometrical factors. Because of the particular topography of the catenand within its iron complexes, formation of octahedral geometries is inhibited. More generally, the entwined topography of the catenate strongly favors low-coordinate complexes versus penta- or hexacoordinate systems.

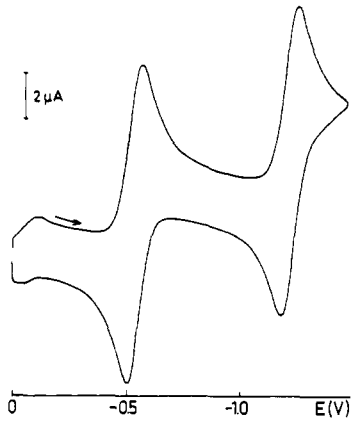

Figure 5. CV of Co·2^{2+} (7×10^{-4} mol L^{-1}) in 0.1 mol L^{-1} DMF–TEAP (HME; scan rate, 100 mV s^{-1}; *E* versus SCE).

As a consequence, high oxidation states, requiring a strong ligand field stabilization, are markedly disfavored as compared to the low ones. However, due to strong topological stabilization, interlocking of the two macrocyclic coordinating subunits precluding easy dissociation of the system, it is still possible to form stable low-coordinate transition-metal complexes in low oxidation states. This is especially well illustrated by the fact that the Fe^{II} complex of **1** could not be obtained.

(c) Cobalt Complexes. Two perfectly reversible one-electron reduction steps are observed for both Co(**1**)$_2^{2+}$ and Co·2^{2+}, in CH_3CN and CH_2Cl_2. The redox potentials of the $Co^{II/I}$ couples are the same (−0.60 V) for both compounds. The only significant difference between the catenate and its open chain analogue is the slightly wider potential stability range of the monovalent cobalt catenate as compared to Co(**1**)$_2^+$. For the catenate, the successive reductions occur at −0.53 V ($Co^{II/I}$) and −1.205 V ($Co^{I/0}$). The corresponding cyclic voltammograms are shown in Figure 5. Comparison of the electrochemical properties of Co(**1**)$_2^{2+}$ and Co·2^{2+} with the previously reported data for cobalt bipy or phen complexes[48-50] shows here again a strong stabilization of the reduced states, Co^{I} and Co^{II}. The same geometrical explanation as previously mentioned, based on the entwined topography of the system, can be put forward. Other sterically constrained polyimine cobalt compounds also lead to stabilized monovalent complexes.[51-53] For instance, the redox potential of the Co(dmbp)$_2^{2+/+}$ couple (dmbp = 6,6′-dimethyl-2,2′-bipyridine) is −0.63 V,[54] showing that in our case their is no particular effect of the interlocked nature of the ligand on the redox potentials. The presence of methyl groups α to the nitrogen atoms of a bipy or phen nucleus is sufficient to prevent formation of tris-chelate compounds and thus to stabilize the monovalent state.[54,55]

Remarkable also is the drastic structural effect of ligands **1** or **2** on the $Co^{III/II}$ redox potential. Whereas bipy or phen complexes of cobalt(II) can very easily be electrochemically oxidized to octahedral cobalt(III),[54,56] the redox potential value of the $Co^{III/II}$ couple being close to 0 V, no oxidation peak is observed for Co·2^{2+} prior to ligand oxidation ($E_p > 1.6$ V). The destabilization effect of cobalt(III) due to entwined or interlocked ligands in complexes of **1** or **2** is thus very large (>1.5 V).

The monovalent complexes Co(**1**)$_2^+$ and Co·2^+ have been prepared by exhaustive electrolysis (at −0.78 V) on a mercury

(39) Tanaka, N.; Sato, Y. *Electrochim. Acta* **1968**, *13*, 335.
(40) Musumeci, S.; Rizzarelli, E.; Sammartano, S.; Bonomo, R. P. *J. Inorg. Nucl. Chem.* **1974**, *36*, 853.
(41) (a) Saji, T.; Aoyagui, S. *J. Electroanal. Chem.* **1975**, *58*, 401. (b) Saji, T.; Aoyagui, S. *J. Electroanal. Chem.* **1975**, *60*, 1.
(42) Morris, D. F.; Hanck, K. W.; De Armond, M. K. *J. Am. Chem. Soc.* **1983**, *105*, 3032.
(43) Floriani, C.; Calderazzo, F. *Coord. Chem. Rev.* **1972**, *8*, 57.
(44) Cohen, I. A.; Ostfeld, D.; Lichtenstein, B. *J. Am. Chem. Soc.* **1972**, *94*, 4522.
(45) Rakowski, M. C.; Busch, D. H. *J. Am. Chem. Soc.* **1975**, *97*, 2570.
(46) Srivatsa, G. S.; Sawyer, D. T.; Boldt, N. J.; Bocian, D. F. *Inorg. Chem.* **1985**, *24*, 2125.
(47) Bard, A. J.; Faulkner, L. R. In *Electrochimie. Principes, Méthodes et Applications*; Masson: Paris, 1983.
(48) Vlček, A. A. *Nature* **1957**, *180*, 753.
(49) Maki, N.; Hirano, T.; Musha, S. *Bull. Chem. Soc. Jpn.* **1963**, *36*, 756.
(50) Tanaka, N.; Sato, Y. *Bull. Chem. Soc. Jpn.* **1968**, *41*, 2059.
(51) Tait, A. M.; Lovecchio, F. V.; Busch, D. R. *Inorg. Chem.* **1977**, *16*, 2206.
(52) Ansell, C. W. G.; Lewis, J.; Liptrot, M. C.; Raithby, P. R.; Schröder, M. *J. Chem. Soc., Dalton Trans.* **1982**, 1593.
(53) Musumeci, S.; Rizzarelli, E.; Sammartano, S.; Bonomo, R. P. *J. Electroanal. Chem.* **1973**, *46*, 109.
(54) Willet, B. C.; Anson, F. C. *J. Electrochem. Soc.* **1982**, *129*, 1260.
(55) Arena, G.; Bonomo, R. P.; Musumeci, S.; Rizzarelli, E. *Z. Anorg. Allg. Chem.* **1975**, *412*, 161.
(56) Chen, Y. W. D.; Santhanam, K. S. V.; Bard, A. J. *J. Electrochem. Soc.* **1982**, *129*, 61.

cathode, in CH_2Cl_2 for **1** and in DMF for **2**. These complexes are deep green, with a very broad absorption band (580–750 nm) in their visible spectrum.

In DMF, stepwise electrolysis of Co·2^{2+} (at −20 °C on Hg pool; small amounts of lutidine present as proton trap) at −0.78 V and later at −1.5 V leads to build-up of the green complex Co·2^{+} at first, followed by subsequent generation of the intense red zerovalent cobalt catenate Co·2^{0}. Coulometric and voltammetric measurements show that these two one electron reductions are quantitative and that the complexes obtained are stable. The starting compound Co·2^{2+} can quantitatively be regenerated from either of its reduced states (formal Co^{I} or Co^{0}) by air or electrochemical oxidation (−0.2 V).

(d) Nickel Complexes. A preliminary account of this study has already been published.[57] A surprising stabilization of monovalent nickel occurs by coordination to **1** or **2**. In CH_3CN, the redox potentials of the Ni^{II}/Ni^{I} couples are −0.16 and −0.18 V for Ni(**1**)$_2^{2+/+}$ and Ni·$2^{2+/+}$, respectively. The same explanation as that put forward for Fe and Co complexes applies to account for the stabilization of Ni^{I} complexes of **1** or **2**. The potential stability range of the nickel(I) catenate (−1.32 to −0.18 V) is remarkably broad.

The behavior of Ni·2^{2+} is strikingly different from that of bipy nickel(II) complexes.[58-60] In the case of unsubstituted bipy ligands, electrochemical reduction of Ni(bipy)$_3^{2+}$ leads directly to Ni(bipy)$_3^{0}$ in a two-electron process ($E_{1/2}$ = −1.3 V).[58] Monovalent nickel is not observed in this latter case.

Electrolysis of Ni(**1**)$_2^{2+}$ or Ni·2^{2+} on Pt generates the corresponding nickel(I) complexes as blue species. [Ni·2^{+}][ClO_4^{-}] can be isolated and recrystallized (CH_2Cl_2–benzene). An EPR study of either Ni(**1**)$_2^{+}$ or Ni·2^{+} clearly shows that those compounds are true d^9 nickel(I) complexes. In many instances, the oxidation state of monovalent complexes containing unsaturated nitrogen ligands is only formal, the redox orbitals involved in the course of the nickel(II) reduction being generally ligand localized.[61,62] In the case of Ni·2^{+}, the g values found (CH_2Cl_2 frozen solution) are g_1 = 2.388, g_2 = 2.143, and g_3 = 2.071. Those data are in good agreement with those previously published for other d^9 Ni^{I} complexes.[63,64]

Due to the almost identical topographical properties of Ni(**1**)$_2^{2+}$ and Ni·2^{2+}, the redox potential values of the corresponding $Ni^{II/I}$ couples are equal. However, the behavior of both compounds with respect to O_2 reoxidation is drastically different. The reactivity of Ni(**1**)$_2^{+}$ is much more pronounced than that of nickel(I) catenate. In CH_2Cl_2, the bimolecular rate constants corresponding to the reaction of the monovalent nickel complex with O_2 are as follows:

$$\text{Ni}(\mathbf{1})_2^{+} + O_2 \xrightarrow{k_{O_2}} \text{products} \qquad k_{O_2} = 2\ M^{-1}\ s^{-1}$$

$$\text{Ni}\cdot\mathbf{2}^{+} + O_2 \xrightarrow{k_{O_2}} \text{products} \qquad k_{O_2} \sim 10^{-5}\ M^{-1}\ s^{-1}$$

The topological properties of Ni·2^{+} (interlocked ligands) have thus a dramatic influence on its kinetic inertness. Although mechanistic considerations regarding the oxidation reaction of both nickel(I) complexes by O_2 would only be speculative at this stage, it is likely that partial dissociation of an intermediate nickel complex is an important step in the course of the reaction. Clearly, this dissociative step is completely inhibited in the catenate, due to the difficulty encountered by the two coordinating subunits in separating.

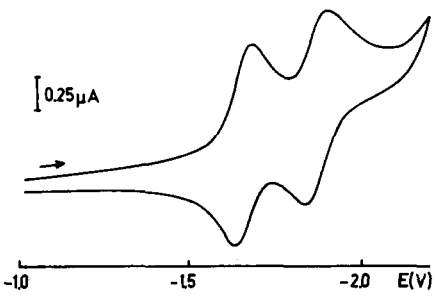

Figure 6. CV of Cu·2^{+} (5.7×10^{-4} mol L^{-1}) in 0.1 mol L^{-1} DMF–TEAP (HME, scan rate, 50 mV s^{-1}; E versus SCE).

As for the iron and cobalt catenates, the tervalent nickel state could not be reached (E_p > 1.4 V for $Ni^{III/II}$).

(e) Copper Complexes. Some preliminary results have already been published.[2]

Oxidation of Copper(I) Complexes. In CH_3CN, Cu(**1**)$_2^{+}$ and Cu·2^{+} are reversibly oxidized to the corresponding divalent complexes in the scan range 30–600 mV s^{-1}. The oxidation potentials are high (~0.6 V versus SCE in CH_3CN), making the copper(II) species Cu(**1**)$_2^{2+}$ and Cu·2^{2+} relatively strong oxidants. The present systems are noticeably different from Cu(bipy)$_2^{+}$ for which the Cu^{II}/Cu^{I} couple has a redox potential value of 0.19 V versus SCE.[65]

The relatively high Cu^{II}/Cu^{I} redox potentials of the presently studied compounds are in good agreement with the previously reported systems: 6,6′-dimethyl-2,2′-bipyridine[33] or 2,9-dimethyl-1,10-phenanthroline complexes.[33,66,67] The particular redox properties of all those Cu^{II}/Cu^{I} couples can be assigned to geometrical factors.[68]

Cu(**1**)$_2^{2+}$ and Cu·2^{2+} are readily and quantitatively electrogenerated from their copper(I) precursors. In the absence of any reducing species, the divalent copper complexes are stable in solution. They are deep green, and they can be crystallized. The low-energy absorption band at 666 nm (ϵ = 820 L mol^{-1} cm^{-1}) is ligand field in nature. It is in agreement with a pseudotetrahedral geometry,[69] as recently reported for another copper(II) complex containing four imidazole groups as ligands[70] and with another Cu^{II} complex of a tetradentate ligand containing a 2,2′-biphenyl spacer.[71]

Reduction of Copper(I) Complexes. The reduction of Cu(**1**)$_2^{+}$ and Cu·2^{+} has been studied in DMF, adsorption phenomena being noticeably more limited than in CH_3CN. Cyclic voltammograms of copper catenate are given in Figure 6. Copper catenate is exceptionally stable. Dissociation does not occur even at a markedly cathodic potentials (~−2 V). This behavior is distinctly different from that of other complexes containing unsubstituted chelates, like bipy and phen. For instance, the following reductive dissociation takes place at −0.62 V.[65]

$$\text{Cu(phen)}_2^{+} \xrightarrow{e^-} 2\text{phen} + \text{Cu}^0_{\text{metal}}$$

In the case of the phen complex, reduction of the monovalent state leads to copper metal, the initial electron transfer occurring either in the Cu 4s orbital or via a phen π^* orbital. Fast dissociation follows this monoelectronic reduction step. For Cu(**1**)$_2^{+}$ and Cu·2^{+}, two reversible one-electron transfers (either on Hg or on Pt) are observed at very negative potentials. The redox orbitals

(57) Dietrich-Buchecker, C. O.; Kern, J. M.; Sauvage, J. P. *J. Chem. Soc., Chem. Commun.* **1985**, 760.
(58) Henne, B. J.; Bartak, D. E. *Inorg. Chem.* **1984**, *23*, 369.
(59) Tanaka, N.; Ogata, T.; Niizuma, S. *Inorg. Nucl. Chem. Lett.* **1972**, *8*, 965.
(60) Troupel, M.; Rollin, Y.; Sock, O.; Meyer, G.; Perrichon, J. *Nouv. J. Chim.* **1986**, *10*, 593.
(61) Lovecchio, F. V.; Gore, E. S.; Busch, D. H. *J. Am. Chem. Soc.* **1974**, *96*, 3109.
(62) Gagnē, R. R.; Ingle, D. M. *Inorg. Chem.* **1981**, *20*, 420.
(63) Ansell, C. W. G.; Lewis, J.; Raithby, P. R.; Ramsden, J. N.; Schröder, M. *J. Chem. Soc., Chem. Commun.* **1982**, 546.
(64) Constable, E. C.; Lewis, J.; Liptrot, M. C.; Raithby, P. R.; Schröder, M. *Polyhedron* **1983**, *2*, 301.
(65) Rastegar, A. Thesis, Louis Pasteur University, Strasbourg, 1985.
(66) Hawkins, C. J.; Perrin, D. D. *J. Chem. Soc.* **1963**, 2996.
(67) Gürtler, O.; Dietz, K. P.; Thomas, Ph. *Z. Anorg. Allg. Chem.* **1973**, *396*, 227.
(68) Sundararajan, S.; Wehry, E. L. *J. Phys. Chem.* **1972**, *76*, 1528 and references cited therein.
(69) Hathaway, B. J. *Struct. Bonding (Berlin)* **1984**, *57*, 55.
(70) Knapp, S.; Keenan, T. P.; Zhang, X.; Fikar, R.; Potenza, J. A.; Schugar, H. J. *J. Am. Chem. Soc.* **1987**, *109*, 1882.
(71) Müller, E.; Piguet, C.; Bernardinelli, G.; Williams, A. F. *Inorg. Chem.* **1988**, *27*, 849.

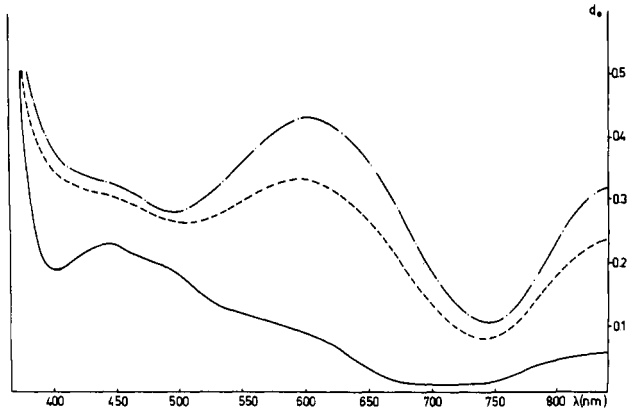

Figure 7. Reduction of Cu·2^{2+}: successive electronic spectra during electrolysis (DMF, −1.73 V, Au grid). t = 0 (—), 25 min (- - -), 90 min (-·-).

involved are likely to be ligand localized, also indicated by the small difference between the redox potentials of the Cu^{I}/Cu^{0} and Cu^{0}/Cu^{-I} couples ($\Delta E_{1/2} \sim 200$ mV)

$$Cu(L)_2^{+} + e^{-} \rightleftharpoons [Cu^{+}(L)(L^{\bullet-})]^{0} \qquad E_{1/2} \sim -1.6 \text{ V}$$

$$[Cu^{+}(L)(L^{\bullet-})] + e^{-} \rightleftharpoons [Cu^{+}(L^{\bullet-})(L^{\bullet-})]^{-} \qquad E_{1/2} \sim -1.8 \text{ V}$$

$$(L)_2 = (\mathbf{1})_2 \text{ or } \mathbf{2}$$

The nature of the redox orbitals is in agreement with previous studies on other transition-metal complexes containing aromatic polyimine chelates as ligands.[72]

Electrolysis of Cu·2^{2+} (DMF, −1.73 V, Pt grid) in the cavity of an EPR spectrometer confirms the radical anion nature of the formally copper(0) complex obtained by one-electron reduction of Cu·2^{2+}: g = 2.000 ± 0.002, ΔH = 39 G.

The reduction potentials of $Cu(\mathbf{1})_2^{+}$ and Cu·2^{2+} are almost identical for both of the formally $Cu^{I/0}$ and $Cu^{0/-I}$ couples but the kinetic stability of the reduced catenate is dramatically more pronounced than that of its acyclic analogue. At low scan rates (<10 mV/s), even the first reduction of $Cu(\mathbf{1})_2^{+}$ becomes irreversible, whereas the corresponding process for Cu·2^{2+} remains completely reversible. Furthermore, the electrochemical reduction of Cu·2^{2+} (DMF, −1.73 V, Au grid, room temperature) allows the buildup of the formally zero-valent complex indicated by a deep-blue solution (λ_{max} = 603 nm, ϵ = 5300 M^{-1} cm^{-1}; λ_{max} = 840 nm, ϵ = 4300 M^{-1} cm^{-1}). The formation of Cu·**2** from Cu·2^{2+} can easily be monitored by electronic spectroscopy as shown in Figure 7. It is noteworthy that, due to the topologically different properties of $Cu(\mathbf{1})_2^{+}$ and Cu·2^{2+}, electrolysis of the former leads only to copper metal and free **1**.

(f) Silver Complexes. The electrochemical study turned out to be especially difficult due to nonreproducible adsorption poisoning phenomena. Redox potentials were determined by polarography using the DME in CH_3CN. The corresponding polarograms are given on Figure 8. The redox potential of free Ag^{+}/Ag at the DME determined in CH_3CN is +0.420 V, in good agreement with previously published data.[73] A noticeable ligand effect is observed for $Ag(\mathbf{1})_2^{+}$ since a significant shift of its reduction potential (235 mV) to less positive values is observed. More remarkable is the behavior of the silver(I) catenate. Its reduction occurs at −0.70 V in CH_3CN and is thus 1.12 V more cathodic than that of free Ag^{+}. Thus, the topological effect estimated by comparing the reduction potential of $Ag(\mathbf{1})_2^{+}$ and Ag·2^{2+} is found to be 0.885 V. The silver(I) catenate Ag·2^{2+} is certainly one of the most difficult silver(I) complexes to reduce. Related to the particular electrochemical stability of Ag·2^{2+} is its highly unusual photochemical inertness. This compound does not darken when stored in daylight for weeks, contrary to the vast majority of other silver(I) complexes or salts.

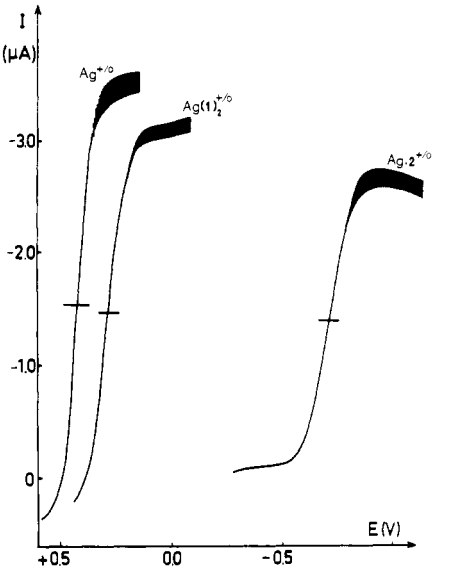

Figure 8. Polarography at the DME of Ag^{+}, $Ag(\mathbf{1})_2^{+}$, and Ag·2^{2+} in 0.1 mol L^{-1} CH_3CN–TEAP (E versus SCE).

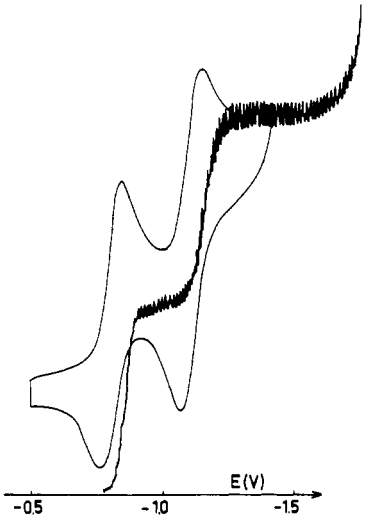

Figure 9. CV on platinum and polarography at the DME of $Zn(\mathbf{1})_2^{2+}$ in 0.1 mol L^{-1} CH_2Cl_2–TBAP (scan rate for CV, 40 mV s^{-1}; E versus $Ag/Ag_3I_4^{-}$).

The surprising electrochemical stability of Ag·2^{2+} may reflect a high formation constant for Ag·2^{2+} as compared to $Ag(\mathbf{1})_2^{+}$, leading to a long-lived reduction product Ag·2^{0}. By comparison, the analogous postulated intermediate for the acyclic complex, $Ag(\mathbf{1})_2^{0}$, is easily formed electrochemically, and it probably rapidly dissociates to **1** and silver(0), the latter subsequently forming silver amalgam.

(g) Zinc Complexes. As the $Zn(\mathbf{1})_2^{2+}$ complex decomposes in DMF, the electrochemical study was carried out in CH_2Cl_2 or CH_3CN. The CV and polarogram of $Zn(\mathbf{1})_2^{2+}$ are shown in Figure 9. The reduction process of both $Zn(\mathbf{1})_2^{2+}$ and Zn·2^{2+} occurs in two one-electron steps in CH_2Cl_2 or in CH_3CN, with a relatively broad (~300-mV) stability range of the formally monovalent zinc complexes. At low scan rate, the CV's are reversible (ΔE_p = 60 mV at v = 20 mV/s), but as the scan rate is increased, ΔE_p increases, indicating a quasi-reversible electron transfer.

Exhaustive electrolysis of Zn·2^{2+} (CH_3CN, Pt) at the first reduction wave plateau (~−1.1 V) leads to formation of a pink–red solution (λ_{max} = 530 nm, $\epsilon \sim$ 1000 L mol^{-1} cm^{-1}) of the monovalent catenate Zn·2^{+}.

EPR measurements performed on a frozen solution of the electrochemically generated monovalent zinc catenate show the

(72) Kaim, W. *Coord. Chem. Rev.* **1987**, *76*, 187 and references cited therein.

(73) Kolthoff, I. M.; Coetze, J. F. *J. Am. Chem. Soc.* **1957**, *79*, 1852.

presence of a radical paramagnetic species (g = 2.00246, ΔH = 11.4 G). The reduced states $Zn{\cdot}2^+$ and $Zn{\cdot}2^0$, containing formally monovalent and zero-valent zinc, respectively, are better described as zinc(II) stabilized anion radicals. Clearly, the redox orbitals involved in the reduction process are ligand localized.

(h) Cadmium Complexes. As for its Zn^{2+} analogue, $Cd(\mathbf{1})_2^{2+}$ is unstable in DMF. The electrochemical study of $Cd(\mathbf{1})_2^{2+}$ and $Cd{\cdot}2^{2+}$ has thus been performed in CH_3CN and CH_2Cl_2. In CH_3CN, free Cd^{2+}, $Cd(\mathbf{1})_2^{2+}$, and $Cd{\cdot}2^{2+}$ are reduced in a two-electron process at −0.285, −0.400, and −0.850 V, respectively.

In each case, the divalent cadmium species is reduced to cadmium amalgam. This is confirmed by electrolysis at fixed potentials of either $Cd(\mathbf{1})_2^{2+}$ or $Cd{\cdot}2^{2+}$: reduction is accompanied by complete demetalation.

In CH_2Cl_2 and on Pt, the electrochemical behavior of $Cd{\cdot}2^{2+}$ is, however, different. The corresponding CV (not shown) indicates that reduction occurs in two steps at −1.15 and −1.36 V. The monovalent and zero-valent complexes could not be built-up in solution. However, it is remarkable that the mono- and direduced cadmium catenates could be observed as transient species when the dissociation reaction is not favored by amalgam formation. Here again, this particular property mainly originates from the interlocking of the ligand since reduction of $Cd(\mathbf{1})_2^{2+}$ under the same conditions leads only to complete dissociation with no observable transient species. At the present stage, it is difficult to know whether the formally cadmium(I) catenate corresponds to a real cadmium(I) complex, analogous to other recently described cage complexes,[74] or to a cadmium(II) stabilized radical anion.

Conclusions

The novel topological properties of the catenand **2** and the concomitant particular entwined shape of its complexes, the catenates, lead to new and surprising effects. A number of catenates, $M{\cdot}2^{n+}$ (M is the cationic species: Cu^{I}, Cu^{II}, Ag^{I}, Co^{II}, Ni^{II}, Zn^{II}, Cd^{II}, and Li^{I}), have been prepared and fully characterized by the usual physical methods. From a preparative viewpoint, several catenates appear to be noticeably more stable than their open-chain analogues with **1**, although the steric and electronic properties of $M{\cdot}2^{n+}$ and $M(\mathbf{1})_2^{n+}$ should be identical. The interlocked nature of **2** is responsible for this enhanced stability, allowing for the preparation of $Zn{\cdot}2^{2+}$, $Cd{\cdot}2^{2+}$, $Li{\cdot}2^{+}$, and $Ni{\cdot}2^{2+}$, whose analogous complexes with **1** could not be isolated in the solid state. ^{1}H NMR spectroscopy clearly shows that, for all the catenates studied, the geometry of the complex is roughly the same: the two dpp subunits are entwined and coordination of the metal occurs via the four nitrogen atoms of the ligand. The pentaoxyethylene fragments have not been found to interact with the complexed species, even in the case of $Li{\cdot}2^{+}$.

The most striking property of the catenand is its ability to stabilize low oxidation states of several transition metals. For instance, the existence range of the monovalent copper(I) catenate $Cu{\cdot}2^{+}$ lies around 2.2 V, both the oxidation and reduction products being still stable in solution. Other examples include $Zn{\cdot}2^{+}$, which can easily be made and studied in solution, and silver(I), which like $Cu{\cdot}2^{+}$ shows an unusually broad redox existence range (−0.7 to ligand oxidation starting around 1.5 V versus SCE). Monovalent cobalt, iron, and nickel catenates, $Co{\cdot}2^{+}$, $Fe{\cdot}2^{+}$, and $Ni{\cdot}2^{+}$, are also highly accessible by reduction, the nickel(I) complex being in addition kinetically inert toward its reoxidation by molecular oxygen. In most cases, comparison of the catenates with their acyclic analogues containing **1** shows a strong contribution of the topological factor of **2** to the ability to stabilize low oxidation states. The enhancement of stability of low oxidation state complexes of catenates as compared to their $M(\mathbf{1})_2^{n+}$ analogues has a profound effect on their kinetic properties. Whereas reduction potential values of $M{\cdot}2^{n+}$ and $M(\mathbf{1})_2^{n+}$ are in several instances very close, the kinetic stability of the reduced catenate with respect to *dissociation* or *reoxidation* is always noticeably more pronounced than that of the corresponding open-chain complex.

Acknowledgment. We thank the CNRS for financial support. Fruitful discussions with Professor P. Federlin and Dr. J. P. Kintzinger are also gratefully acknowledged. We also thank Dr. J. J. Andrē and M. Bernard for EPR spectra.

Registry No. **1**, 89333-97-1; $Co(\mathbf{1})_2^{2+}$, 121704-89-0; $Co(\mathbf{1})_2^{+}$, 121704-96-9; $Co(\mathbf{1})_2$, 121704-97-0; $Ni(\mathbf{1})_2^{2+}$, 98987-66-7; $Ni(\mathbf{1})_2^{+}$, 98987-65-6; $Ni(\mathbf{1})_2$, 121705-00-8; $Cu(\mathbf{1})_2^{2+}$, 121705-02-0; $Cu(\mathbf{1})_2^{+}$, 95246-98-3; $Cu(\mathbf{1})_2$, 121705-03-1; $Cu(\mathbf{1})_2^{-}$, 121705-04-2; $Zn(\mathbf{1})_2^{2+}$, 121730-26-5; $Zn(\mathbf{1})_2^{+}$, 121705-07-5; $Zn(\mathbf{1})_2$, 121705-08-6; $Ag(\mathbf{1})_2^{+}$, 121704-84-5; $Ag(\mathbf{1})_2$, 121705-11-1; $Cd(\mathbf{1})_2^{2+}$, 121704-91-4; $Cd(\mathbf{1})_2$, 121705-13-3; $Li{\cdot}2^{+}$, 121704-88-9; **Li·2**, 121704-92-5; $Li{\cdot}2^{-}$, 121704-93-6; $Fe{\cdot}2^{2+}$, 121704-94-7; $Fe{\cdot}2^{+}$, 121730-27-6; **Fe·2**, 121704-95-8; $Co{\cdot}2^{2+}$, 121704-90-3; $Co{\cdot}2^{+}$, 121704-98-1; **Co·2**, 121704-99-2; $Ni{\cdot}2^{2+}$, 99919-65-0; $Ni{\cdot}2^{+}$, 99919-56-9; **Ni·2**, 121705-01-9; $Cu{\cdot}2^{2+}$, 121704-83-4; $Cu{\cdot}2^{+}$, 88503-31-5; **Cu·2**, 121705-05-3; $Cu{\cdot}2^{-}$, 121705-06-4; $Zn{\cdot}2^{2+}$, 121704-86-7; $Zn{\cdot}2^{+}$, 121705-09-7; **Zn·2**, 121705-10-0; $Ag{\cdot}2^{+}$, 121704-85-6; **Ag·2**, 121705-12-2; $Cd{\cdot}2^{2+}$, 121704-87-8; $Cd{\cdot}2^{+}$, 121705-14-4; **Cd·2**, 121705-15-5; **2**, 90030-13-0; $H{\cdot}2^{+}$, 108703-53-3.

(74) Lardinois, P.; Rebena, I.; Hickel, B. *New J. Chem.* **1988**, *12*, 21.
(75) Gutman, V.; Schmid, R. *Monatsh. Chem.* **1969**, *100*, 2113.

Detection of Alkylperoxo and Ferryl, $(Fe^{IV}{=}O)^{2+}$, Intermediates during the Reaction of *tert*-Butyl Hydroperoxide with Iron Porphyrins in Toluene Solution

Ramesh D. Arasasingham, Charles R. Cornman, and Alan L. Balch*

Contribution from the Department of Chemistry, University of California, Davis, California 95616. *Received December 12, 1988*

Abstract: PFe^{II} and $PFe^{III}OH$ (P is a porphyrin dianion) catalyze the decomposition of *tert*-butyl hydroperoxide in toluene solution without appreciable attack on the porphyrin ligand. ^{1}H NMR spectroscopic studies at low temperature (−70 °C) give evidence for the formation of a high-spin, five-coordinate intermediate, $PFe^{III}OOC(CH_3)_3$. On warming this decomposes to $PFe^{III}OH$ (P = tetramesitylporphyrin, TMP) or $PFe^{III}OFe^{III}P$ (P = tetra-*p*-tolylporphyrin, TTP) with the formation of $(TMP)Fe^{IV}{=}O$ as an observed intermediate in the first case. Treatment of $PFe^{III}OOC(CH_3)_3$ at −70 °C with *N*-methylimidazole (MeIm) yields the intermediate $(MeIm)PFe^{IV}{=}O$. Organic products formed from this reaction are *tert*-butyl alcohol, di-*tert*-butyl peroxide, benzaldehyde, acetone, and benzyl-*tert*-butyl peroxide, which arise largely from a radical chain process initiated by the iron porphyrin but continuing without its intervention.

The peroxidase, catalase, and cytochrome P-450 enzymes utilize alkyl hydroperoxides to generate high-valent oxoiron porphyrins.[1-3] Extensive studies on the peroxidase-catalyzed oxidations have established that the enzyme reacts with hydroperoxides to form

0002-7863/89/1511-7800$01.50/0